structure was determined by direct methods. Refinement of two blocks (190 + 32 parameters), 4217 unique reflections, and 1923 reflections with $I > 1.5\sigma(I)$ has an agreement value, R, currently at 0.23. Two unidentified solvent molecules seem to be present in each asymmetric unit (32 in the unit cell).

Equilibrium Constant Measurements. NMR solvents used in equilibrium constant measurement were purchased from Aldrich as the highest atom % deuterated compounds in a glass vial, i.e., $(CD_3)_2CO$, 100.0% atom D; CD_3CN, 100.0% atom D; C_6D_6, 100.0% atom D; ClC_6D_5, 98.5% atom D; $(CD_2)_6$, 99.5% atom D; $(CD_3)_2NCDO$, 99.5% atom D; C_2D_5OD, anhydrous, 99+% atom D; $(CD_2)_4O$, 99.5% atom D; $CD_3C_6D_5$, 100.0% atom D; $CDCl_3$, 100.0% atom D; CD_2Cl_2, 100.0% atom D and CCl_4, which was distilled from P_2O_5, and were opened under argon prior to preparing NMR samples.

Samples were weighed on a microbalance, Mettler Instrument (1 div = 0.1 mg). The sample was dissolved in 0.5 mL or 1.0 mL of deuterated solvent in a 5-mm NMR tube. Relatively concentrated NMR samples higher than 1.0 mM concentration were prepared by weighing solid samples, transferring into a NMR tube, drying the NMR tube in a pistol under high vacuum at 60 °C overnight, filling the pistol with argon, followed by adding the NMR solvent to the NMR tube under argon by syringe. The NMR sample was stored in a refrigerator. The dilute samples (concentration <1.0 mM stock solution) were prepared from a 1.0 mM stock solution. Specific amounts of 1.0 mM stock solution were transferred into a NMR tube by a microsyringe. The sample in the tube was concentrated to dryness by flowing argon gas into the tube. The NMR tube was then dried in a pistol, and the procedures were followed as described above.

The ^1H NMR spectra were recorded on a Bruker AM 500 at 500 MHz. The temperature was measured at desired points on the scale by using a MeOH-temperature calibrating sample. For comparison of data at specific temperatures, generally 30 °C to -50 °C, temperatures over 5 or 10 °C intervals were used. The temperature was calculated from observed chemical shift difference due to CH_3 and OH resonances by using the following equation:[24]

$$T(K) = 403 - \frac{29.5}{M}\Delta\nu - \frac{23.81}{M^2}(\Delta\nu)^2$$

where M is the spectrometer frequency (Hz) and $\Delta\nu$ is the chemical shift difference between CH_3 and OH resonances (Hz). The peaks employed were integrated with ±10% error.

Supplementary Material Available: Table I, association constants for homodimerization in $CDCl_3$, and Table II, association constants for heterodimerization in $CDCl_3$, section on known bridging compounds, systematic names, syntheses, and full characterizations of **7** and **9–15**, and structure of FMeNPz **19** (15 pages). Ordering information is given on any current masthead page.

Constrictive and Intrinsic Binding in a Hemicarcerand Containing Four Portals[1,2]

Donald J. Cram,* Michael T. Blanda, Kyungsoo Paek, and Carolyn B. Knobler

Contribution from the Department of Chemistry and Biochemistry, University of California at Los Angeles, Los Angeles, California 92004. *Received April 1, 1992*

Abstract: The synthesis, crystal structure, and binding properties are reported for a globe-shaped hemicarcerand (**4**) composed of two rigid bowl-like units (polar caps) attached to one another at their rims through four *o*-xylyl units (equatorial spacers). Four pendant β-phenylethyl groups attached to each of the polar caps impart solubility to the system. The critical shell-closing reaction, $2Ar(OH)_4 + 4\,o\text{-}C_6H_4(CH_2Br)_2$ (+ base) → $Ar(OCH_2C_6H_4CH_2O)_4Ar$, went in 20–25% yields in $(CH_3)_2NCOCH_3$ as solvent, one molecule of which is a template for the eight bond-forming reactions and becomes a guest in the hemicarceplex, stable at 25 °C. In the crystal structure of the complex, the guest is disordered, and one polar cap is rotated 21° about the polar axis with respect to the other polar cap. This rotation minimizes the internal volume and surface area of the system and closes the portals. When heated at 100 °C in a series of solvents whose volumes and shapes are complementary to those of the inner phase of **4**, complex **4**·$(CH_3)_2NCOCH_3$ underwent guest exchange with solvent to give **4**·solvent at 100–120 °C; the exchange rate decreased in the following sequence of solvents used: $C_6D_5Br \geq C_6D_5Cl >$ 1,2-$(CD_3)_2C_6D_4 > C_6D_5CD_3 >$ 1,4-$CD_3C_6D_4CD_3 > Cl_2CDCDCl_2$. Empty host **4** in differing maximum amounts was detected as an intermediate in these guest substitution reactions. First-order rates for guest loss to solvent in $CDCl_2CDCl_2$ at 100 °C decreased with guest change as follows: $CH_3CN > (CH_3)_2NCOCH_3 \approx (CH_3)_2NCHO > C_6H_5CH_3 \approx$ MeCOEt > BuOH > $CHCl_2CHCl_2$ > EtOAc. Solvents too large to enter **4** were *o*-$(CH_3)_2C_6H_4$, *m*-$(CH_3)_2C_6H_4$, *p*-$CH_3C_6H_4CH_2CH_3$, *p*-$(CH_3CH_2)_2C_6H_4$, *p*-$CH_3C_6H_4CH(CH_3)_2$, $(CH_3)_3CC_6H_5$, 1,3,5-$(CH_3)_3C_6H_3$, and *p*-$(CH_3)_2CHC_6H_4CH(CH_3)_2$. Heating **4**·$(CH_3)_2NCOCH_3$ in *p*-$(CH_3)_2CHC_6H_4CH(CH_3)_2$ to 160 °C for 24 h produced empty **4**, which in 1,2-$(CD_3)_2C_6D_4$ at temperatures ranging from 80 to 130 °C was submitted to in and out rate measurements (^1H NMR) with $(CH_3)_2NCOCH_3$, $CH_3CH_2O_2CCH_3$, $CH_3CH_2COCH_3$, and $C_6H_5CH_3$ as guests. Association constants, $\Delta G°$, ΔH, ΔS, $\Delta G^{\ddagger}_{in}$, and $\Delta G^{\ddagger}_{out}$ were calculated and are discussed in terms of intrinsic and constrictive free energy contributions to the activation free energies for dissociation. With $CH_3CH_2O_2CCH_3$, $(CH_3)_2NCOCH_3$, and $CH_3CH_2COCH_3$, the associations were both enthalpy and entropy driven to provide $-\Delta G°$ values at 100 °C of 3.8, 3.7, and 5.3 kcal mol^{-1}, respectively. With $C_6H_5CH_3$, the complexation was entropy driven, but enthalpy opposed to give a $-\Delta G°$ value (100 °C) of 3.4 kcal mol^{-1}. These effects are interpreted in terms of the relative rigidities of the guests, the liberation of complexing solvent upon incarceration, the conversion of *inner consolidated* into *dispersed outer space* of the host upon complexation, and host-guest attractive forces between complexing partners.

In prior papers of this series, we reported the syntheses and binding properties of two types of hemicarcerands. The first type[3,4] was composed of two polar caps possessing C_4 axes attached to one another with three short spacer units [$(OCH_2O)_3$], leaving a fourth possible position as a portal for entry or egress of potential guests (**1**). The inner space of this host proved to have unique properties of constraining or enhancing (depending on spacial relationships) conformational reorganizations of guests, of providing a nonsolvating environment for carrying out chemical reactions,[3,4] and as a phase in which cyclobutadiene could be synthesized and preserved at room temperature.[5] The second type of hemicarcerand (**2**) made use of the same polar caps coupled

(1) Host–Guest Complexation. 63.

(2) We warmly thank the U.S. Public Health Services for supporting Grant GM-12640 and the National Science Foundation for supporting Grant NSF CHE 8802800.

(3) Tanner, M. E.; Knobler, C. B.; Cram, D. J. *J. Am. Chem. Soc.* **1990**, *112*, 1659–1660.

(4) Cram, D. J.; Tanner, M. E.; Knobler, C. B. *J. Am. Chem. Soc.* **1991**, *113*, 7717–7727.

(5) Cram, D. J.; Tanner, M. E.; Thomas, R. *Angew. Chem., Int. Ed. Engl.* **1991**, *30*, 1024–1027.

0002-7863/92/1514-7765$03.00/0

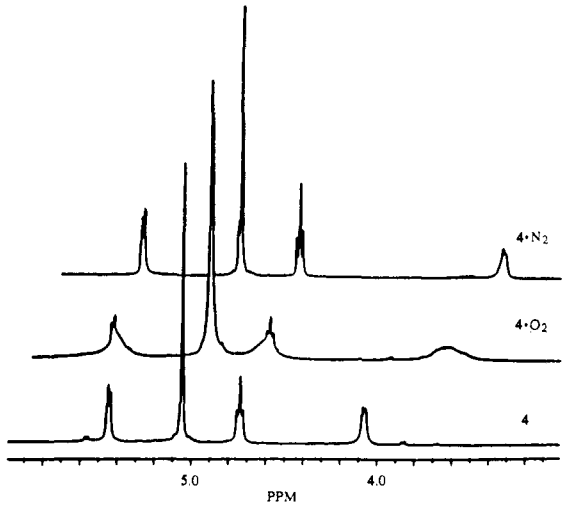

Figure 1. Effect of saturating $CDCl_2CDCl_2$ solutions of **4** with oxygen (**4**·O_2) or nitrogen (**4**·N_2) on the 500-MHz ^1H NMR spectrum of the substance at 25 °C. Spectra are offset by 0.2 ppm upfield for clarity.

with one another through four rigid spacer units [(1,3-CH=N-C_6H_4N=CH)$_4$], which provided four portals and an inner-phase volume large enough to accommodate the respective entrance and occupancy of guest molecules as large as [2.2]paracyclophane, ferrocene, adamantane, and camphor.[6] The hemicarceplexes of both types of hosts were stabilized enough by constrictive binding to allow their isolation and characterization by standard techniques.

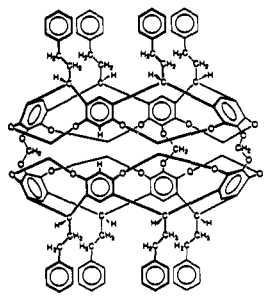

1

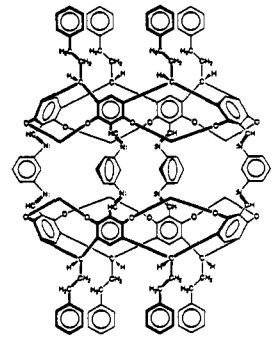

2

The present paper reports the synthesis, crystal structure, and binding properties of hemicarcerand **4** containing the same two polar caps and eight solubilizing appended $C_6H_5CH_2CH_2$ groups as in **1** and **2**, but with four semimobile equatorial spacer groups [1,2-($OCH_2C_6H_4CH_2O$)] connecting the two polar caps. Unlike those of **1** and **2**, CPK models of **4** indicate that, when the polar caps are perfectly aligned one over the other, the portals are open and are large enough to allow models of molecules as large as *p*-xylene to enter and egress the inner phase of the hemicarcerand. If one polar cap of the model of **4** is rotated with respect to the other around the polar axis, the portals close, the polar caps approach one another, the inner volume decreases, and many new atom-to-atom close contacts are formed.

The study of **4** was undertaken to answer the following questions. (1) Do the polar caps of **4** rotate with respect to one another as is suggested by model examination? (2) To what extent does incarceration restrict the molecular rotations of incarcerated guests? (3) What is the mechanism of guest substitution in these hemicarceplexes? (4) Is **4** capable of constrictively binding appropriately shaped guests? (5) What structural recognition does **4** exhibit in the complexation of various families of guests? (6) What are the relationships between guest structure and the free energies of complexation? (7) How do the activation free energies for dissociation of complexing partners partition between overcoming constrictive vs intrinsic binding? (8) How do complexation activation free energies depend on guest structures? (9) How does partitioning of the free energies of binding between enthalpic vs entropic terms depend on the guest structures? This type of host is new and, therefore, these questions have never been asked before.

(6) Quan, M. L. C.; Cram, D. J. *J. Am. Chem. Soc.* **1991**, *113*, 2754.

Results

Syntheses. Tetrol **3** was synthesized as before[4] in a five-step (three-pot) sequence in 23% yield from resorcinol and hydrocinnamaldehyde as primary starting materials. The shell closure of 4 mol of 1,2-($BrCH_2$)$_2C_6H_4$ with 2 mol of **3** in $(CH_3)_2NCOCH_3$–Cs_2CO_3 went in 23% yield to give **4**·$(CH_3)_2NCOCH_3$, which was easily purified by chromatography and crystallization. This

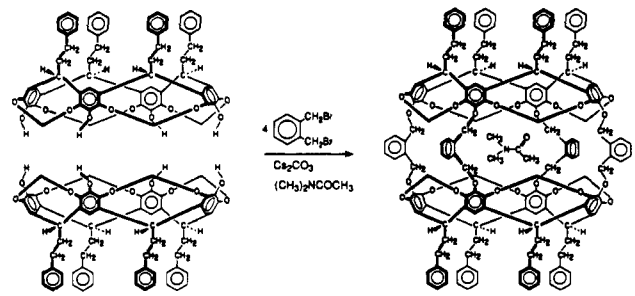

3 **4**·$(CH_3)_2NCOCH_3$

hemicarceplex was stable to ordinary laboratory manipulations at temperatures below 70 °C and was stable indefinitely at 25 °C and below. The compound was fully characterized by elemental analysis, ^1H NMR, and FAB-MS. The free host was prepared by heating this complex to 160 °C for 24 h in 1,4-[$(CH_3)_2CHC_6H_4CH(CH_3)_2$], a solvent which in CPK models is much too large to be incarcerated in **4**. Free host **4** was also fully characterized. Its FAB-MS gave a 10% peak (**4**, 100%) corresponding to **4**·H_2O. When dissolved in $CDCl_2CDCl_2$, **4** partially and rapidly formed **4**·O_2 and **4**·N_2 when O_2 and N_2 were bubbled through the solution, respectively. The ^1H NMR spectrum of **4** is very sensitive to the presence of these guests in the interior of the host. In particular, the δ value of the eight inward-facing OCH_2O protons (Figure 1) moves upfield by 0.12 ppm in the solution of O_2 and by 0.27 ppm in the solution of N_2. The coalescence temperatures for **4**·N_2 and **4**·O_2 appear to be below room temperature. The two complexes can be rapidly interconverted by simply passing a stream of the new gas into a solution of the one to be displaced. As noted with **1**,[4] this phenomenon provides a useful diagnostic test for empty **4**.

Crystal Structure of 4·$(CH_3)_2NCOCH_3$·(solvate)$_n$. Crystallization of **4**·$(CH_3)_2NCOCH_3$ from $(CH_3)_2NCOCH_3$–$CHCl_3$–O-$(CH_2CH_2)_2O$ gave crystals which contained as many as 18 disordered solvent molecules per host, one being the incarcerated $(CH_3)_2NCOCH_3$, the others being present as solvates. This disorder inhibited refinement of the crystal structure past the *R* value of 0.30. Although poor, the structure of the host that emerged is good enough for the purposes of this paper. Scheme I contains a stereodrawing (**5**) of the crystal structure in which the disordered guest and solvate molecules are omitted.

The (1,2-$OCH_2C_6H_4CH_2O$)$_4$ connecting units in the equatorial region of the hemicarceplex assume a conformation in which the northern polar cap is rotated by 21° with respect to the southern polar cap about a C_2 polar molecular axis. Each set of the four $ArOCH_2Ar$ oxygens attached to each polar cap forms a near-square plane (±0.04 Å, least squares). The two squares are ~2.4 Å apart and are close to being parallel to one another, as is shown by the fact that the angle between the normals to these least-squares planes is 0.6°. The distance between the two oxygen atoms common to each *o*-xylyl bridge varies between 2.76 and 2.95 Å. The electron pairs of all eight oxygen atoms face toward the inner phase of the host, and their attached *o*-xylyl groups face outward. The aryls of the xylyl groups are arranged in a manner which provides the host with a C_2 rather than a C_4 polar axis. Their

Table I. Effect of Guest Changes on the ^{1}H NMR Spectral Chemical Shifts ($CDCl_3$, 500 MHz, 25 °C) of the Inward-Turned OCH_2O Protons in Hemicarceplexes of Host **4**

guest	obsd δ	$\Delta\delta$	guest	obsd δ	$\Delta\delta$
none	4.08	0	$C_6H_5CH_3$	4.16	+0.08
$(CH_3)_2NCOCH_3$	4.20	+0.12	$C_6H_5C_2H_5$	4.02 (4.16)	−0.06 (+0.08)
$(CH_3)_2NCHO$	3.95	−0.13	1,4-$(CH_3)_2C_6H_4$	4.16	+0.08
CH_3CN	3.82	−0.26	$CHCl_3$	3.87	−0.21
$CH_3(CH_2)_3OH$	4.10	+0.02	$CHCl_2CHCl_2$	4.09	+0.01
$CH_3CH_2COCH_3$	3.89	−0.19	O_2	3.95	−0.13
$CH_3CH_2O_2CCH_3$	4.02 (4.15)	−0.06 (+0.07)	N_2	3.81	+0.27
$(CH_2)_4O$	3.89	−0.19			

Scheme I

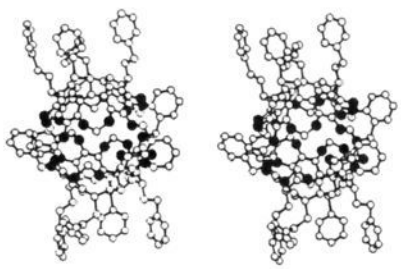

5, stereoview of ordered part of crystal structure of **4**

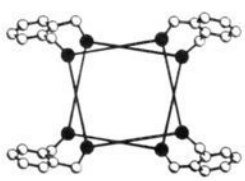

6, parallel squares formed by oxygens of bridges

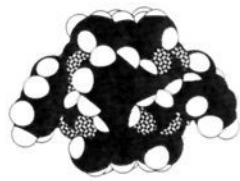

7, computer-drawn structure of **5** minus the eight $CH_2CH_2C_6H_5$ groups

arrangement, the two squares defined by the eight $ArOCH_2Ar$ groups, and the twist of the two polar caps are visualized in partial structure **6** of Scheme I. Also included in Scheme I is a computer drawing **7** of hemicarcerand **4** minus its eight appended $C_6H_5CH_2CH_2$ groups. This drawing approximates CPK models of the same structure and is based on the crystal structure coordinates.[7] *This structure, unlike the ball and stick representations of the* crystal structure (**5**), shows how the polar twist closes the portals and increases the number of close contacts between atoms of the rims of the polar caps and those of the equatorial spacer groups.

Guest Variation in Hemicarceplexes. Twelve different hemicarceplexes were prepared and characterized in which different guests were incarcerated in **4**. The new complexes were obtained either directly from **4**·$(CH_3)_2NCOCH_3$ or from preformed empty **4**. In the former method, **4**·$(CH_3)_2NCOCH_3$ was heated at 80–200 °C in the new guest as solvent or cosolvent, and the guest-substitution reaction was driven to completion by mass action. Typically, aromatic or halogenated solvents such as $C_6H_5CH_3$ or $CHCl_2CHCl_2$ readily dissolved **4**·$(CH_3)_2NCOCH_3$, whereas more polar solvents such as CH_3CN, $CH_3(CH_2)_3OH$, $CH_3COCH_2CH_3$, and $CH_3CH_2O_2CCH_3$ did not. Of the five equimolar solvent mixtures of $C_6H_5CH_3$ with five more polar solvents ($(CH_2)_4O$, CH_3CN, $CH_3(CH_2)_3OH$, $CH_3CH_2COCH_3$, and $CH_3CH_2O_2CCH_3$) that were examined, only the first led to a mixture of complexes (85:15, **4**·$(CH_2)_4O$–**4**·$C_6H_5CH_3$). In the other four cases, only the complexes of the smaller, more polar guests were formed under conditions of kinetic control of products. Prolonged heating of these mixtures eventually led to equilibrated mixtures of two complexes.

The geometric constraints of the portal through which guests had to pass during entry into or egress from the inner phase of **4** were probed by heating either **4** or **4**·$(CH_3)_2NCOCH_3$ to high temperatures using as solvent guests of increasing size and differing shapes. The largest molecules that formed detectable complexes were $C_6H_5CH_2CH_3$, 1,4-$CH_3C_6H_4CH_3$, and $CHCl_2CHCl_2$. No complexes were detected with the following compounds as guests: 1,2-$CH_3C_6H_4CH_3$, 1,3-$CH_3C_6H_4CH_3$, $(CH_3)_3CC_6H_5$, 1,4-$CH_3C_6H_4C_2H_5$, 1,4-$C_2H_5C_6H_4C_2H_5$, 1,4-$CH_3C_6H_4CH(CH_3)_2$, 1,3,5-$(CH_3)_3C_6H_3$, and 1,4-$(CH_3)_2CHC_6H_4CH(CH_3)_2$. A sharp discontinuity depending on the shape of the guest is evident in the complexation of *p*-xylene and the lack of complexation of *o*-xylene and *m*-xylene. As expected on the basis of CPK molecular model examination, ethylbenzene readily complexes with **4**. Fully characterized complexes include **4**·$(CH_3)_2NCOCH_3$, **4**·$(CH_3)_2NCHO$, **4**·CH_3CN, **4**·$CH_3(CH_2)_3OH$, **4**·$CH_3CH_2COCH_3$, **4**·$CH_3CH_2O_2CCH_3$, **4**·$(CH_2)_4O$, **4**·$C_6H_5CH_3$, **4**·$C_6H_5CH_2CH_3$, **4**·1,4-$CH_3C_6H_4CH_3$, **4**·$CHCl_3$, and **4**·$CHCl_2CHCl_2$.

Solution ^{1}H NMR Spectra of 4 and Derived Carceplexes. Since the rates of decomplexation of all guests examined except O_2 and N_2 were on the order of 10^{-6} s^{-1} at 25 °C, ^{1}H NMR spectroscopy proved to be very valuable for determining the presence of guest in host and the stoichiometry of complexation. For all guests examined except O_2 and N_2, the complexes were one-to-one, a conclusion supported by their elemental analyses.

Table I indicates the effect of guests on the 500-MHz ^{1}H NMR spectral chemical shifts in $CDCl_3$ at 25 °C of the inward-turned OCH_2O protons in each of the two hemispheres of the hemicarceplexes of **4**. Two different kinds of signals were observed for this type of proton only when the guest was $CH_3CH_2O_2CCH_3$ or $C_6H_5CH_2CH_3$ at room temperature. The two kinds of signals indicate that at 25 °C the long axes of these two guests are aligned with the long north–south axis of the host and that these guests do not rotate end-to-end (around east–west axes) rapidly on the ^{1}H NMR time scale. The presence of only one kind of host signal in complexes containing the other non-like-ended guests such as $(CH_3)_2NCOCH_3$, $(CH_3)_2NCHO$, CH_3CN, $CH_3CH_2CH_2CH_2OH$, $CH_3COCH_2CH_3$, $(CH_2)_4O$, and $C_6H_5CH_3$ suggests that these guests do rotate end-to-end rapidly on the ^{1}H NMR time scale.

Three complexes were subjected to temperature-dependent spectral studies. When taken at −80 °C, the spectrum of **4**·CH_3CN showed little change, demonstrating that even at this temperature the guest rotations around all axes were rapid on the spectral time scale. The spectrum of **4**·$C_6H_5CH_3$ changed with cooling to provide a coalescence temperature (T_c) at −9 °C (and a $\Delta\nu$ = 60 Hz), giving $\Delta G^{\ddagger}$ = 13 kcal mol^{-1} for end-to-end rotation of the guest relative to the host.[8] The spectrum of **4**·$CH_3CH_2O_2CCH_3$ coalesced at 100 °C ($\Delta\nu$ = 60 Hz) to provide $\Delta G^{\ddagger}$ = 18 kcal mol^{-1} for a similar rotation.[8] Molecular model examination of **4**·$C_6H_5CH_3$ and **4**·$CH_3CH_2O_2CCH_3$ suggests that these rotations must occur when the host is in an unwrapped conformation in which the guests are much less closely held. Thus part of the activation energy for end-to-end rotations of these guests must involve overcoming the attractions of the bridging atoms for one another in their wrapped conformation. Smaller

(7) (a) We warmly thank Dr. Robert Thomas for generating this drawing. (b) We warmly thank Mr. Joey Storer for drawing and minimizing the energy for this unwrapped structure.

(8) Oki, M. *Applications of Dynamic NMR Spectroscopy to Organic Chemistry*; Marchand, A. P., Ed.; VCH Publishers, Inc.: Deerfield Beach, FL, 1985; Vol. 4, pp 1–50.

Table II. Spectral Changes (^{1}H NMR, $CDCl_3$, 500 MHz, 25 °C) in Chemical Shifts of Guest Proton Caused by Guest Incarceration in **4**

guest	proton	δ (ppm) free (type)	δ (ppm) bound (type)	Δδ
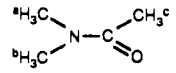	H^a	2.95 (s)	1.20	1.75
	H^b	3.05 (s)	−1.15	4.20
	H^c	2.10 (s)	−2.19	4.29
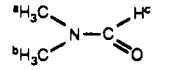	H^a	2.90 (s)	−0.45 (s)	3.35
	H^b	2.95 (s)	0.04 (s)	2.91
	H^c	8.00 (s)	4.77 (s)	3.23
$H_3{}^aCCN$	H^a	2.05 (s)	−2.55 (s)	4.50
$CH_3{}^aCH_2{}^bCH_2{}^cCH_2{}^dOH^e$	H^a	0.95 (t)	−2.90 (t)	3.85
	H^b	1.2–1.9 (bm)	−0.55 (m)	1.75–2.6
	H^c	1.2–1.9 (bm)	−0.70 (m)	1.75–2.6
	H^d	3.65 (m)	1.00 (m)	2.65
	H^e	2.18 (t)	−2.21 (t)	4.39
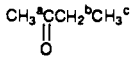	H^a	2.10 (s)	−2.00 (s)	4.10
	H^b	2.35 (q)	0.06 (q)	2.29
	H^c	1.05 (t)	−2.90 (t)	3.95
$CH_3{}^aCH_2{}^bO_2CCH_3{}^c$	H^a	1.25 (t)	−2.34 (t)	3.59
	H^b	4.10 (t)	2.00 (q)	2.10
	H^c	2.08 (s)	−2.13 (s)	4.21
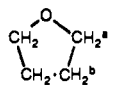	H^a	3.70 (bm)	0.27 (bm)	3.43
	H^b	1.85 (bm)	−0.97 (bm)	2.82
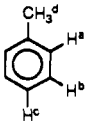	H^a	7.20 (bs)	5.39–5.40 (d)	1.80
	H^b	7.20 (bs)	4.78 (t)	2.42
	H^c	7.20 (bs)	2.81 (t)	4.39
	H^d	2.38 (s)	−1.93 (s)	4.31
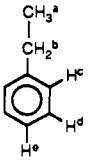	H^a	1.20 (t)	−2.89 (t)	4.09
	H^b	2.65 (q)	0.80 (q)	2.73
	H^c	7.10 (bs)	5.85 (d)	1.25
	H^d	7.10 (bs)	4.70 (t)	2.30
	H^e	7.10 (bs)	3.00 (t)	4.10
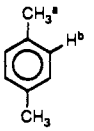	H^a	2.30 (s)	−1.87 (s)	4.17
	H^b	6.98 (s)	5.96 (s)	1.02
Cl_3CH^a	H^a	7.26 (s)	5.29 (s)	1.97
$Cl_2CH^aCHCl_2$	H^a	6.00 (s)	4.20 (s)	1.80

guests such as CH_3CN or $CHCl_3$ can probably rotate without such unwrapping, whereas 1,4-$CH_3C_6H_4CH_3$ and $CHCl_2CHCl_2$ are probably incapable of end-to-end rotations (model examination) at ordinary working temperatures.

Interestingly, six of the fourteen complexes of Table I contain guests that move the inward-turned host OCH_2O protons upfield ($\Delta\delta$ is negative), six move the protons downfield ($\Delta\delta$ is positive), and the two that provide two signals each move one upfield and the other downfield of the signals of empty **4**. The larger less polar guests are associated with the lower field shift, and the more polar guests provide the higher field shifts.

Table II records the ^{1}H NMR (500 MHz, 25 °C) spectral chemical shifts of complexed and uncomplexed guests, the proton assignments, and the $\Delta\delta$ values (ppm) due to incarceration of the guests. Generally, the guest protons were shifted upfield by 1–4 ppm from their normal positions due to their presence in a magnetically anisotropic environment composed largely of the faces of benzene rings in the polar caps and OCH_2O and OCH_2Ar groups in the respective temperate and torrid zones. The time-averaged positions of the various guest protons suggested by CPK model examination are roughly borne out by the magnitudes of the $\Delta\delta$ values coupled with the expectation that in terms of shielding power: polar caps > temperate zone > equatorial zone. The longest and most tightly held rigid guest is 1,4-$CH_3C_6H_4CH_3$, whose methyl protons certainly occupy the polar caps ($\Delta\delta$ = 4.17) and whose ArH atoms occupy the torrid zone ($\Delta\delta$ = 1.02). The terminal protons of the long axis of toluene must occupy the terminal caps, since they exhibit the large upfield shifts of $\Delta\delta$ = 4.31 ($CH_3{}^d$) and $\Delta\delta$ = 4.39 (ArH^c), as compared to $\Delta\delta$ = 2.42 for H^b protons and $\Delta\delta$ = 1.80 for H^a (see Table II). The terminal protons of $C_6H_5CH_2CH_3$, H^a and H^e, are pressed into the polar caps as shown by their $\Delta\delta$ values of 4.09 and 4.10 ppm, respectively, while their H^b and H^d protons occupy the temperate zone ($\Delta\delta$ = 2.73 and 2.30, respectively) and H^c the torrid zone ($\Delta\delta$ = 1.25). The smaller and more mobile but rigid $(CH_2)_4O$ guest provides $\Delta\delta$ = 3.43 for its H^a and $\Delta\delta$ = 2.82 ppm for its H^b protons. As expected from model examination, the H^a protons α to the oxygen can penetrate more deeply into the polar cap than can H^b, since O is smaller than CH_2. The rigid $(CH_3)_2NCOCH_3$ guest has its two methyls lying on the longest molecular axis (H^b and H^c protons) occupying the polar caps to provide $\Delta\delta$ values of 4.20 and 4.29 ppm, respectively, whereas the H^a proton of the remaining methyl is located in the temperate zone ($\Delta\delta$ = 1.75 ppm). All protons of $(CH_3)_2NCHO$ provide lower $\Delta\delta$ values (3.35–2.91 ppm) due to its greater mobility and shift-averaging ability associated with its much less than complete occupation of the inner phase of **4**. This result contrasts with the fact that bound CH_3CN provides the highest $\Delta\delta$ value (4.5 ppm) and yet is the smallest guest in Table II. We attribute this to location of the slightly acidic protons of the CH_3CN molecule contacting the four aryl groups composing a polar cap, which acts as a π-base complementary to the protons.

As expected from the general parallel alignment of the long axes of host and guest in the complexes, the terminal protons of the aliphatic guests have higher $\Delta\delta$ values than the internal protons. Thus, H^a and H^e of $CH_3(CH_2)_3OH$ exhibit $\Delta\delta$ = 3.85 and 4.39

Table III. Pseudo-First-Order Rate Constants for Disappearance of 4·$(CH_3)_2NCOCH_3$ in a Series of Deuterated Solvents at 100 °C

solvent	maximum % of free **4**	k_1 ($s^{-1} \times 10^4$)
C_6D_5Br	3	93
C_6D_5Cl	4	83
1,2-$(CD_3)_2C_6D_4$	100	8.5
1,4-$(CD_3)_2C_6D_4$	8	3.5
$CDCl_2CDCl_2$	45	2.6
$C_6D_5CD_3$	<1	2.0

ppm, respectively, whereas H^b, H^c, and H^d provide $\Delta\delta$ values lying between 1.75 and 2.65. The terminal H^a and H^c protons of $CH_3COCH_2CH_3$ have respective $\Delta\delta$ values of 4.10 and 3.95 ppm, whereas that for H^b lies at 2.29 ppm. The terminal H^a and H^c protons of $CH_3CH_2O_2CCH_3$ have respective $\Delta\delta$ values of 3.59 and 4.21, while that of H^b is 2.10.

Mechanism of Guest Substitution by New Guest in Hemicarceplexes. When a sample of 4·$(CH_3)_2NCOCH_3$ was heated in an ^1H NMR tube at 100 °C with a potential new guest as solvent, the ^1H NMR spectra of the host over time displayed the original spectrum plus the growth of two new spectra and finally the disappearance of the original and one of the two new spectra. The transient spectrum was determined to be that of empty **4**, and the final spectrum to be that of the new hemicarceplex in which a solvent molecule was substituted for the original guest. Table III records the pseudo-first-order rate constants for disappearance of 4·$(CH_3)_2NCOCH_3$ in the six deuterated solvents: C_6D_5Br, C_6D_5Cl, 1,2-$(CD_3)_2C_6D_4$, 1,4-$(CD_3)_2C_6D_4$, $C_6D_5CD_3$, and $CDCl_2CDCl_2$. Also included is the maximum percentage of free host which accumulated in the run (1,2-$(CD_3)_2C_6D_4$ does not enter **4**).

These results clearly indicate that substitution occurs by a two-step mechanism in which the first step is decomplexation to give the empty hemicarcerand, which in a second step becomes complexed with a solvent molecule. The low concentration of

$$4\cdot(CH_3)_2NCOCH_3 \xrightarrow{k_1} \mathbf{4} + (CH_3)_2NCOCH_3 \xrightarrow[\text{solvent}]{k_2} \mathbf{4}\cdot\text{solvent} \quad (1)$$

initial guest produced compared to solvent (factor of about 4000) should render the dissociation effectively irreversible. The data indicate the decomplexation rate constant (k_1) for 4·$(CH_3)_2NCOCH_3$ going to **4** is solvent dependent. The solvents decrease in the following order in their abilities to promote decomplexation: $C_6D_5Br \geq C_6D_5Cl >$ 1,2-$(CD_3)_2C_6D_4 >$ 1,4-$(CD_3)_2C_6D_4 \geq C_6D_5CD_3 > CDCl_2CDCl_2$, with the total spread being a factor of 150. This difference must be associated with the ability of the solvents to differentially solvate the transition states for decomplexation. Molecular model (CPK) examination of possible transition states indicates that the complex must be in an extended (unwrapped) conformation in which the cross section of three possible portals is minimized so that the cross section of the portal employed for guest passage can be maximized. The different shapes and polarizabilities of the solvents must control the extent to which they can solvate the ground state and the transition states involved in these decomplexations, both for host and guest.

Survey of the Dependence of Decomplexation Rates of 4·Guest on Guest Structure. Table IV records the first-order rate constants for decomplexation of 10 different hemicarceplexes in $CDCl_2CDCl_2$ at 100 °C. The hemicarceplexes all have **4** as their host and differ widely in their guests. The total spread in passing from the highest rate constant observed for CH_3CN to the lowest rate constant (for $CH_3CH_2O_2CCH_3$) is only a factor of 15. The guests, when arranged in decreasing order of their rate constants for decomplexation, are as follows: $CH_3CN > (CH_3)_2NCHO > (CH_3)_2NCOCH_3 > (CH_2)_4O > C_6H_5CH_3 > CH_3(CH_2)_3OH > CH_3CH_2COCH_3 > CHCl_2CHCl_2 > CH_3CH_2O_2CCH_3$. This order obviously reflects a composite of effects, such as guest size, shape, and conformational flexibility, as well as the electronic character of the atoms and functional groups involved.

Table IV. Dependence of Decomplexation Rates on Guest Structure of 4·Guest in $CDCl_2CDCl_2$ at 100 °C

guest	$t_{1/2}$ (min)	k_1 ($s^{-1} \times 10^4$)
CH_3CN	38	3.0
$(CH_3)_2NCHO$	42	2.7
$(CH_3)_2NCOCH_3$	45	2.6
$(CH_2)_4O$	87	1.3
$CH_3C_6H_5$	209	0.55
$CH_3(CH_2)_3OH$	260	0.44
$CH_3CH_2COCH_3$	308	0.39
$CHCl_2CHCl_2$	352	0.33
$CH_3CH_2O_2CCH_3$[a]	409	0.28

[a] Estimated from rate constant at 130 °C assuming it decreased by a factor of 3 in going to 100 °C, as was observed in $(CD_3)_2C_6D_4$ as solvent (see Table V).

Chart I. Close Contacts (+0.1 Å of van der Waals)

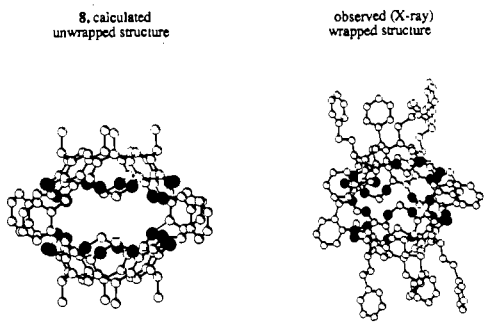

O···O	3.1	4	4
O···C	3.3	15	37
C···C	3.5	12	27
	sums	31	68

Δ = 37 close contacts associated with wrapping

It is interesting that the solvent effects on decomplexation rates should be a power of 10 more important than the guest structural effects. We interpret this relationship as reflecting the fact that the host reorganization of wrapping and unwrapping involves the loss of many close contacts between atoms on the bowl rims and on the bridging *o*-xylyl units. Essentially the same activation energy cost has to be paid before guests as small as CH_3CN or as large as $CHCl_2CHCl_2$ can escape incarceration and probably does not differ greatly with guest size once a guest the size of CH_3CN is reached. The high sensitivity of the decomplexation rate to the solvent structure implies that, in the transition state for complexation–decomplexation, guest–solvent contacts are energetically important. Thus, the transition state possesses a structure in which the guest is just starting to exchange host–guest interactions for solvent–guest attractions. In other words, the transition-state structure more resembles that of the starting materials than it does the structure of the hemicarceplex.

Chart I provides views of **4** in its unwrapped (extended) state (**8**) (energy minimized) and in its wrapped (crystal structure **5**) state. The close contacts (+0.1 Å of van der Waals distance[9]) for each conformation are listed and summed. Those of the wrapped conformation exceed those of the unwrapped by 37 and are of the O···C (Δ = 22) and C···C (Δ = 15) varieties. In other work, we found a rough correlation between the number of intermolecular close contacts of a similar variety generated in complexes in $CDCl_3$ formed by 4-fold "lock and key" dimers,[10] whose binding free energies in $CDCl_3$ in some cases were >9 kcal mol^{-1}.

Kinetic and Thermodynamic Parameters for Association and Dissociation of Hemicarceplexes 4·Guest in 1,2-$(CD_3)_2C_6D_4$.

(9) Bondi, A. *J. Phys. Chem.* **1964**, *68*, 441–451.
(10) Cram, D. J.; Choi, H. J.; Bryant, J. A.; Knobler, C. B. *J. Am. Chem. Soc.*, in press.

Table V. Kinetics of Association and Dissociation Involving Hemicarceplexes 4·Guest in 1,2-$(CD_3)_2C_6D_4$

guest	temp (K)	k_a (min^{-1} M^{-1})	k_d (min^{-1} × 10^2)	K_a (M^{-1} × 10^{-2})
$(CH_3)_2NCOCH_3$	353	2.1	1.2	1.78
$(CH_3)_2NCOCH_3$	373	8.0	5.1	1.57
$(CH_3)_2NCOCH_3$	393	26	18.7	1.40
$CH_3CH_2O_2CCH_3$	373	0.25	0.14	1.79
$CH_3CH_2O_2CCH_3$	393	0.76	0.52	1.44
$CH_3CH_2O_2CCH_3$	403	1.7	1.3	1.30
$CH_3COCH_2CH_3$	323	0.055	0.0025	22.0
$CH_3COCH_2CH_3$	333	0.089	0.0046	19.4
$CH_3COCH_2CH_3$	353	0.36	0.023	15.9
$CH_3COCH_2CH_3$	373[a]	1.44[a]	0.11[a]	13.00[a]
$C_6H_5CH_3$	353	0.062	0.084	0.73
$C_6H_5CH_3$	373	0.32	0.34	0.95
$C_6H_5CH_3$	403	1.33	1.20	1.10

[a] Values extrapolated to 373 K.

Mixtures containing 5:1 or 10:1 ratios of guest to empty host at 2 mM concentration in 1,2-$(CD_3)_2C_6D_4$ were prepared in NMR tubes, which were heated in the probe of a 500-MHz NMR spectrometer. Series of 20–25 ^1H NMR spectra were acquired over time at three temperatures (±1 °C) for each host–guest combination. The temperature of the probe was calibrated against an ethylene glycol standard.[11] Concentrations of the free host and complexes were determined by integrating proton signals unique to each. Calculated second-order rate constants are recorded in Table V.

Decomplexation first-order kinetics was followed in the same solvent at similar concentrations and temperatures. A series of 20–25 spectra were recorded over time. The ratios of free host to complex were determined from the integrations of the inward-pointing protons of the OCH_2O groups. Table V records the first-order rate constants obtained and the calculated association (K_a) constants at three different temperatures for each of the four guests $(CH_3)_2NCOCH_3$, $CH_3CH_2O_2CCH_3$, $CH_3COCH_2COCH_3$, and $C_6H_5CH_3$.

Table VI records the $\Delta G°$, ΔH, ΔS, $\Delta G^{‡}_{assoc}$, $\Delta H^{‡}_{assoc}$, $\Delta S^{‡}_{assoc}$, $\Delta G^{‡}_{dissoc}$, $\Delta H^{‡}_{dissoc}$, and $\Delta S^{‡}_{dissoc}$ values calculated in the usual way from the rate and equilibrium constants and the temperature dependence.

Constrictive and Intrinsic Binding. We define constrictive binding as being $\Delta G^{‡}_{dissoc} - (-\Delta G°)$, which equals $\Delta G^{‡}_{assoc}$, the free energy of the transition state for association relative to the free energy of the uncomplexed state. Thus, constrictive binding refers to the free energy which must be provided to reach the transition state for dissociation from the associated state, minus the intrinsic binding free energy of the binding partners ($-\Delta G°$). Since $\Delta G_{constrictive}$ is taken from an activation free energy term, it is positive.

Interestingly, the constrictive binding free energies ($\Delta G^{‡}_{assoc}$) that must be overcome for 4·guest to dissociate vary little with guest structure changes: for $(CH_3)_2NCOCH_3$, 23.5; for $CH_3CH_2O_2CCH_3$, 25.9; for $CH_3CH_2COCH_3$, 24.8; and for $C_6H_5CH_3$, 25.8 kcal mol^{-1}. We conclude that most of the constrictive binding is associated with the host reorganizing from a highly wrapped structure (with a minimum internal volume and many close contacts between the bridging groups and the rims of the caps) to an unwrapped structure in which the cross section of one portal is maximized and many close contacts are lost. Thus, the energetics of constructive binding are much more controlled by the structure of the common host 4 than by the structures of the four different guests. As the guests become progressively larger (possibly with $CHCl_2CHCl_2$), this generalization probably will not apply.

The values for the intrinsic binding ($\Delta G°$) at 100 °C vary with guest structure as follows: $(CH_3)_2NCOCH_3$, −3.7; $CH_3CH_2O_2CCH_3$, −3.9; $CH_3CH_2COCH_3$, −5.3; and $C_6H_5CH_3$, −3.4 kcal mol^{-1}. Notice that the intrinsic binding free energies correlate inversely with guest size: $CH_3CH_2COCH_3$ (5 heavy atoms) > $CH_3CH_2O_2CCH_3$ (6 heavy atoms) > $(CH_3)_2NCOCH_3$ (6 heavy atoms) > $C_6H_5CH_3$ (7 heavy atoms). The first three of the guests contain C=O dipoles, whose positive carbon atoms are electronically complementary to the 16 inward-turned unshared electron pairs of the host's 8 $ArOCH_2$ oxygens. Also, these three guests all have enthalpic (ΔH) contributions to the binding free energies that are negative: $CH_3CH_2O_2CCH_3$, −3.1; $CH_3CH_2COCH_3$, −2.5; and $(CH_3)_2NCOCH_3$, −3.7 kcal mol^{-1}. Their corresponding entropic contributions ($-T\Delta S$) to the intrinsic binding free energies are also negative: $CH_3CH_2O_2CCH_3$, −0.75; $CH_3CH_2COCH_3$, −2.8; and $(CH_3)_2NCOCH_3$, −2.2 kcal mol^{-1}. Thus, the intrinsic binding energies for these three guests are both enthalpically and entropically driven.

In contrast, the $\Delta G°$ value for 4 binding $C_6H_5CH_3$ is −3.4 kcal mol^{-1}, being opposed by ΔH (+2.2 kcal mol^{-1}) and driven by $-T\Delta S$ (−5.6 kcal mol^{-1}). We attribute the unfavorable enthalpy of binding of $C_6H_5CH_3$ by 4 to be due to the lack of complementarity in shape between the extensive flat surfaces of $C_6H_5CH_3$ and the curved surfaces of the interior of 4. Accordingly, 4·$C_6H_5CH_3$ has few host–guest close contacts. In contrast, the flat surfaces of the 1,2-$(CD_3)_2C_6D_4$ solvent should provide many close contacts between $C_6H_5CH_3$ in its dissociated state.

Entropic Driving Forces for Intrinsic Binding. The entropies of binding all guests have positive signs for the formation of 4·guest, which is highly unusual for processes in nonpolar solvents in which two molecules are collected and their movements restricted relative to one another. Positive entropies as high as 6 cal mol^{-1} K^{-1} have been observed by Collet for a cryptophane complex with CH_2Cl_2,[12] and we have observed entropies as high as 40 cal mol^{-1} K^{-1} for dimerization of certain velcrands in $CDCl_3$.[10] We interpret the present case as reflecting two additive effects. Solvated guest releases solvent molecules that become part of the medium, thereby driving the complexation process. This solvophobic driving force for complexation has been often observed in hydroxylic solvents (mainly water) but seldom in hydrocarbon solvents.

The second effect reflects the entropy of dilution of empty space.[10,13] An empty host such as 4 possesses an inner space of substantial size. When a guest such as $C_6H_5CH_3$ enters the interior of 4, much of the empty space gathered in the interior of 4 is displaced by the guest, and it becomes dispersed into many smaller spaces throughout the solvent, driven by entropic dilution. In other words, large empty spaces in the interior of hemicarcerands are broken into many small empty spaces and scattered throughout the bulk solvent phase, which contributes to the overall fluidity of the liquid. Thus, entropic driving forces for complexation can be observed even in hydrocarbon solvents.

Enthalpic Contributions to Constrictive Binding. Table VI lists the $\Delta H^{‡}$ and $\Delta S^{‡}$ values for association of empty 4 with four different guests to form the transition states for complexations. The respective enthalpic ($\Delta H^{‡}$, kcal mol^{-1}) and entropic ($-T\Delta S^{‡}$, kcal mol^{-1} at 373 K) contributions to $\Delta G^{‡}_{assoc}$ for the four complexes are as follows: 16.3 vs 7.2 for $(CH_3)_2NCOCH_3$; 19.2 vs 6.7 for $CH_3CH_2O_2CCH_3$; 17.7 vs 7.1 for $CH_3CH_2COCH_3$; and 20.7 vs 5.1 for $C_6H_5CH_3$. Thus, for all four guests, $\Delta H^{‡}$ and $-T\Delta S^{‡}$ components for the constrictive binding are positive. The enthalpic contribution varies from 69 to 80% of the total constrictive binding, while the entropic contributions vary from 31 to 20% with changes in the guest structure. The entropic contribution to this transition-state barrier is the lowest (20%) for $C_6H_5CH_3$ as guest, the only one free of conformational mobility which likely would be frozen out in the transition state for complexation.

Summary. A new hemicarcerand host 4 has been designed and synthesized, and the crystal structure of 4·$(CH_3)_2NCOCH_3$ was determined. The hemicarceplexes are composed of two rigid polar

(11) Van Geet, A. L. *Anal. Chem.* **1968**, *40*, 2227–2229.

(12) Collet, A. *Angew. Chem., Int. Ed. Engl.* **1989**, *28*, 1246–1248.

(13) (a) Cram, D. J.; Stewart, K. D.; Goldberg, I.; Trueblood, K. N. *J. Am. Chem. Soc.* **1985**, *107*, 2574–2575 and references contained within. (b) Stein, M. L.; Reisse, J. *Calorim. Anal. Therm.* **1984**, *15*, 214–219.

Table VI. Thermodynamic and Kinetic Parameters for Association and Dissociation Involving Hemicarceplexes 4·Guest in 1,2-$(CD_3)_2CC_6D_4$ at 100 °C

				association			dissociation		
guest	$\Delta G°$ (kcal mol^{-1})	ΔH (kcal mol^{-1})	ΔS (cal K^{-1} mol^{-1})	$\Delta G^{\ddagger}$ (kcal mol^{-1})	$\Delta H^{\ddagger}$ (kcal mol^{-1})	$\Delta S^{\ddagger}$ (cal K^{-1} mol^{-1})	$\Delta G^{\ddagger}$ (kcal mol^{-1})	$\Delta H^{\ddagger}$ (kcal mol^{-1})	$\Delta S^{\ddagger}$ (cal K^{-1} mol^{-1})
$(CH_3)_2NCOCH_3$	−3.7	−1.5	+6	23.5	16.3	−19.4	27.2	20.5	−18.3
$CH_3CH_2O_2CCH_3$	−3.8	−3.1	+2	25.9	19.2	−17.9	29.8	22.2	−23.1
$CH_3COCH_2CH_3$	−5.3	−2.5	+7.5	24.8	17.7	−19.0	30.1	20.8	−25.3
$C_6H_5CH_3$	−3.4	+2.2	+15	25.8	20.7	−13.6	29.2	14.3	−40.0

caps attached to one another at their rims by four equatorially located 1,2-$(OCH_2)_2C_6H_4$ spacer groups. The two caps are rotated with respect to one another by about 21° around the polar axis, which closes the four portals in the equatorial region of the globe. When heated to 100 °C in solvents complementary to the inner phase of **4**, 4·$(CH_3)_2NCOCH_3$ gave 4·solvent by a mechanism involving free **4** as an intermediate. The guest exchange reactions were driven by mass law. Structural recognition for incarceration was illustrated by the fact that 1,4-$(CH_3)_2C_6H_4$ is readily complexed whereas 1,2-$(CH_3)_2C_6H_4$ and 1,3-$(CH_3)_2C_6H_4$ are not. Rate constants for associations and dissociations and equilibrium constants were determined in 1,2-$(CD_3)_2C_6D_4$ for 4·guest at different temperatures with four different guests: CH_3CH_2CO-CH_3, $CH_3CH_2O_2CCH_3$, $(CH_3)_2NCOCH_3$, and $C_6H_5CH_3$. Intrinsic free energies of binding ($\Delta G°$) at 100 °C varied from −3.4 to −5.3 kcal mol^{-1} and contained substantial entropic (solvophobic) driving forces for association. The constrictive binding free energies ($\Delta G^{\ddagger}_{assoc}$) varied from 23.5 to 25.9 kcal mol^{-1}l and were composed of about 25 ± 5% entropic and 75 ± 5% enthalpic driving forces.

Experimental Section

General Procedures. All chemicals were reagent grade and used directly unless otherwise noted. All reactions were conducted under an atmosphere of argon, unless indicated otherwise. Tetrahydrofuran (THF) was freshly distilled from sodium benzophenone ketyl just prior to use. Dimethylformamide (DMF) and dimethylacetamide (DMA) were dried by storage for >72 h over activated (24 h, 320 °C) 3-Å molecular sieves and were degassed under high vacuum just before use. In all procedures involving $CHCl_3$ with uncomplexed **4**, the solvent was passed through a plug of silica gel prior to use to remove ethanol. A Bruker AM-500 spectrometer was used to record ^{1}H NMR spectra. Spectra taken in $CDCl_3$ were referenced to residual $CHCl_3$ at 7.26 ppm. Those spectra taken in $CDCl_2CDCl_2$ were referenced to $CHCl_2CHCl_2$ at 5.99 ppm. Spectra taken in 1,2-$(CD_3)_2C_6D_4$ were referenced to 1,2-$(CH_3)_2C_6H_4$ at 2.25 ppm. NMR samples that were saturated with a gas were prepared by passing a stream of the desired gas through the sample for a minimum of 10 min. Degassed NMR samples were prepared by freezing the samples in liquid nitrogen, evacuating to 0.1 Torr, and thawing. This procedure was repeated three times, and on the final cycle, the tube was sealed prior to thawing. FAB-MS spectra were determined on a ZAB SE instrument. NOBA, as a matrix, stands for 3-nitrobenzyl alcohol. Gravity chromatography was performed on E. Merck silica gel 60 (70–230 mesh). Thin-layer chromatography was performed on glass-backed plates (silica gel 60, F_{245}, 0.25 mm).

36,51-(Epoxymethano[1,2]benzenomethanoxy)-22,26:61,65-dimethano-2,56:19,31-dimetheno-3,55,18,32-(methynoxymethano[1,2]benzenomethanoxymethyno)-1*H*,20*H*,28*H*,30*H*,57*H*,59*H*-bis[1,3]benzodioxocino[9′,8′-*d*′]dibenzo[8,9:21,22]bis[1,3]benzodioxocino[9′,10′:17,18;10″,9‴:25,26][1,3,6,11,14,16,19,24]octaoxacyclohexacosino[4,5-*j*:13,12-*j*′]bis[1,3]benzodioxocin, 8,13,41,46-Tetrahydro-1,20,28,30,57,59,67,92-octakis(2-phenylethyl), Stereoisomer, $(CH_3)_2NCOCH_3$ Complex [4·$(CH_3)_2NCOCH_3$]. Benzenetetrol (1 g, 1 mmol) and α,α-dibromo-*o*-xylene (1 g, 4 mmol) were dissolved in 100 mL of dry, degassed DMA. This solution was added dropwise, via syringe, over 8 h to a stirred mixture of 500 mL of DMA and 7 g of Cs_2CO_3 heated to 60 °C. After 24 h, an additional 4 mmol of the dibromide dissolved in 100 mL of DMA was added to the reaction vessel over the same time period. The reaction was stirred for 24 h after the second addition, making the total reaction time approximately 60 h. The DMA was evaporated under reduced pressure, and the residue was redissolved in $CHCl_3$. The solution was filtered through Celite to remove the carbonate base. The filtrate was concentrated to 50 mL and poured into 400 mL of vigorously stirred methanol. After 30 min, the precipitate that formed was filtered and chromatographed on silica gel with 3% EtOAc in $CHCl_3$ as the eluant (R_f = 0.5). Recrystallization of the column residue from $CHCl_3$–hexanes yielded 290 mg (23%) of 4·$(CH_3)_2NCOCH_3$. The sample was dried at 160 °C for 12 h at 5 × 10^{-5} Torr: ^{1}H NMR (500 MHz, $C_2D_2Cl_4$) δ −2.19 (s, 3 H, $CH_3NCH_3COCH_3$), −1.15 (s, 3 H, $CH_3NCH_3COCH_3$), 1.20 (s, 3 H, $CH_3NCH_3COCH_3$), 2.40–2.78 (m, 32 H, CH_2CH_2Ph), 4.19–4.20 (d, 8 H, inner OCH_2, J = 5 Hz), 4.85 (t, 8 H, methine, J = 7.5 Hz), 5.10 (s, 16 H, benzylic), 5.46–5.47 (d, 8 H, outer OCH_2, J = 5 Hz), 6.95 (s, 8 H, ArH), 7.21–7.43 (m, 56 H, ArH); MS (FABS, NOBA) *m/e* 2527 (M, 100), 2440 (empty **4**, 75). Anal. Calcd for $C_{164}H_{145}NO_{25}$: C, 77.87; H, 5.73. Found: C, 77.92; H, 5.61.

Empty 4. Approximately 20 mg of 4·$(CH_3)_2NCOCH_3$ was dissolved in 50 mL of 1,4-diisopropylbenzene. The solution was degassed by the freeze–pump–thaw cycle (three times) and sealed under vacuum. The solution was heated to 160 °C for 48 h and then cooled to 25 °C. The sealed tube was opened and isooctane was added until a white solid precipitated from solution. This solid was filtered and dried: ^{1}H NMR for free **4** (500 MHz, $C_2D_2Cl_4$) δ 2.45–2.75 (m, 32 H, CH_2CH_2Ph), 4.08–4.09 (br d, 8 H, inner OCH_2), 4.75 (t, 8 H, methine, J = 7.5 Hz), 5.06 (s, 16 H, benzylic), 5.43–5.44 (d, 8 H, outer OCH_2, J = 5 Hz), 6.71 (s, 8 H, ArH), 7.21–7.43 (m, 56 H, ArH); MS (FABS, NOBA) *m/e* 2458 (H_2O + **4**, 10), 2440 (empty **4**, 100). Anal. Calcd for $C_{160}H_{136}O_{24}$: C, 78.69; H, 5.57. Found: C, 78.82; H, 5.55.

4·O_2. Approximately 7 mg of **4** was dissolved in 0.5 mL of degassed $CDCl_2CDCl_2$ in a standard NMR tube. Oxygen gas was bubbled into the solution for 15 min, and the ^{1}H NMR spectrum was recorded immediately afterward: ^{1}H NMR for 4·O_2 (500 MHz, $C_2D_2Cl_4$) δ 2.47–2.77 (m, 32 H, CH_2CH_2Ph), 3.95 (br, 8 H, inner OCH_2), 4.60 (br t, 8 H, methine), 5.06 (br s, 16 H, benzylic), 5.50–5.52 (br d, 8 H, outer OCH_2), 6.75 (br s, 8 H, ArH), 7.21–7.43 (m, 56 H, ArH). No further characterization was attempted.

4·N_2. Into the O_2-saturated solution described above was bubbled N_2 gas for 15 min, and the ^{1}H NMR spectrum was recorded immediately: ^{1}H NMR for 4·N_2 (500 MHz, $C_2D_2Cl_4$) δ 2.40–2.78 (m, 32 H, CH_2CH_2Ph), 3.81–3.82 (d, 8 H, inner OCH_2, J = 5 Hz), 4.75 (t, 8 H, methine, J = 7.5 Hz), 5.00 (s, 16 H, benzylic), 5.61–5.62 (d, 8 H, outer OCH_2, J = 5 Hz), 6.95 (s, 8 H, ArH), 7.21–7.43 (m, 56 H, ArH). No further characterization was attempted.

4·1,4-$(CH_3)_2C_6H_4$. Approximately 20 mg of 4·$(CH_3)_2NCOCH_3$ (0.007 mmol) was dissolved in 25 mL of *p*-xylene. The solution was heated to reflux (138 °C) for 48 h and cooled to 25 °C. The 4·1,4-$(CH_3)_2C_6H_4$ that formed was precipitated from solution by the addition of isooctane, collected, and dried: ^{1}H NMR for 4·1,4-$(CH_3)_2C_6H_4$ (500 MHz, $C_2D_2Cl_4$) δ −1.87 (s, 6 H, CH_3PhCH_3), 2.40–2.78 (m, 32 H, CH_2CH_2Ph), 4.14–4.15 (d, 8 H, inner OCH_2, J = 5 Hz), 4.98 (s, 16 H, benzylic), 5.06 (t, 8 H, methine, J = 7.5 Hz), 5.48–5.49 (d, 8 H, outer OCH_2, J = 5 Hz), 5.96 (d, 4 H, ArH, *p*-xylene, J = 3.5 Hz), 7.13 (s, 8 H, ArH of host), 7.35–7.60 (m, 56 H, ArH); MS (FABS, NOBA) *m/e* 2546 (M, 100), 2440 (empty **4**, 65). Anal. Calcd for $C_{168}H_{146}O_{24}$: C, 79.18; H, 5.73. Found: C, 78.96; H, 5.38.

4·$CH_3CH_2C_6H_5$. Approximately 20 mg of 4·$(CH_3)_2NCOCH_3$ was dissolved in 30 mL of ethylbenzene and was heated to reflux (136 °C) for 48 h. The mixture was cooled to 25 °C and isooctane was added to precipitate the new complex. The complex was filtered and dried: ^{1}H NMR for 4·$CH_3CH_2C_6H_5$ (500 MHz, $C_2D_2Cl_4$) δ −2.89 (t, 3 H, CH_3CH_2Ph, J = 7 Hz), 0.80 (q, 2 H, CH_3CH_2Ph, J = 7 Hz), 2.40–2.80 (m, 32 H, CH_2CH_2Ph), 3.0 (t, 1 H, ArH of EtC_6H_5), 4.02–4.03 (d, 4 H, inner OCH_2, southern hemisphere, J = 5 Hz), 4.15–4.16 (d, 4 H, inner OCH_2, northern hemisphere, J = 5 Hz), 4.70 (t, 2 H, ArH of EtC_6H_5, J = 3 Hz), 4.75–4.80 (d of t, 8 H, methine, J = 7.5 Hz), 5.02 (s, 8 H, benzylic, southern hemisphere), 5.03 (s, 8 H, benzylic, northern hemisphere), 5.48–5.49 (d, 4 H, outer OCH_2, southern hemisphere, J = 5 Hz), 5.56–5.57 (d, 4 H, outer OCH_2, northern hemisphere, J = 5 Hz), 5.85 (d, 2 H, ArH of EtC_6H_5, J = 3 Hz), 6.82 (s, 4 H, ArH, southern hemisphere), 6.83 (s, 4 H, ArH of northern hemisphere), 7.21–7.63 (m, 56 H, ArH); MS (FABS, NOBA) *m/e* 2546 (M, 100), 2440 (empty **4**, 40). Anal. Calcd for $C_{168}H_{146}O_{24}$: C, 79.18; H, 5.73. Found: C, 79.36; H, 5.82.

4·$CH_3C_6H_5$. Approximately 20 mg of 4·$(CH_3)_2NCOCH_3$ was dissolved in 30 mL of $CH_3C_6H_5$ and heated to reflux (110 °C) for 48 h. The mixture was cooled to 25 °C, isooctane was added, and the precipitate was filtered and dried: ^{1}H NMR for 4·$CH_3C_6H_5$ (500 MHz, $C_2D_2Cl_4$) δ −1.93 (s, 3 H, CH_3Ph), 2.50–2.77 (m, 32 H, CH_2CH_2Ph), 2.81 (t, 1 H, ArH of toluene, J = 3.5 Hz), 3.87–3.88 (d, 8 H, inner

OCH_2, J = 5 Hz), 4.71 (t, 2 H, ArH of toluene, J = 3.5 Hz), 4.78 (t, 8 H, methine, J = 7.5 Hz), 4.96 (s, 16 H, benzylic), 5.25–5.26 (d, 8 H, outer OCH_2, J = 5 Hz), 5.39–5.40 (d, 2 H, ArH of toluene, J = 3.5 Hz), 6.93 (s, 8 H, ArH), 7.19–7.34 (m, 56 H, ArH); MS (FABS, NOBA) m/e 2532 (M, 100), 2440 (empty **4**, 60). Anal. Calcd for $C_{167}H_{144}O_{24}$: C, 79.15; H, 5.68. Found: C, 79.08; H, 5.66.

4·$(CH_2)_4O$. A solution of 20 mg of **4**·$(CH_3)_2NCOCH_3$ in 40 mL of THF was heated to reflux (65 °C) for 4 days. Isooctane was added, and the complex was filtered and dried: ^{1}H NMR for **4**·$(CH_2)_4O$ (500 MHz, $C_2D_2Cl_4$) δ −0.97 (m, 4 H, CH_2 α to O in THF), 0.27 (m, 4 H, CH_2CH_2 of THF), 2.40–2.78 (m, 32 H, CH_2CH_2Ph), 3.88–3.89 (d, 8 H, inner OCH_2, J = 5 Hz), 4.68 (t, 8 H, methine, J = 7.5 Hz), 5.04 (s, 16 H, benzylic), 5.80–5.81 (d, 8 H, outer OCH_2, J = 5 Hz), 6.83 (s, 8 H, ArH), 7.17–7.40 (m, 56 H, ArH); MS (FABS, NOBA) m/e 2513 (M^+, 100), 2440 (empty **4**, 50). Anal. Calcd for $C_{164}H_{144}O_{25}$: C, 78.34; H, 5.73. Found: C, 78.62; H, 5.83.

4·$CHCl_2CHCl_2$. A solution of 20 mg of **4**·$(CH_3)_2NCOCH_3$ in 20 mL of tetrachloroethane was heated to 120 °C for 48 h, and the solution was cooled to 25 °C. Isooctane was added, and the precipitate was filtered and dried: ^{1}H NMR for **4**·$CHCl_2CHCl_2$ (500 MHz, $C_2D_2Cl_4$) δ 2.48–2.68 (m, 32 H, CH_2CH_2Ph), 4.09–4.10 (d, 8 H, inner OCH_2, J = 5 Hz), 4.20 (s, 2 H, $Cl_2CHCHCl_2$), 4.90 (t, 8 H, methine, J = 7.5 Hz), 5.08 (s, 16 H, benzylic), 5.49–5.50 (d, 8 H, outer OCH_2, J = 5 Hz), 6.98 (s, 8 H, ArH), 7.20–7.38 (m, 56 H, ArH); MS (FABS, NOBA) m/e 2608 (M, 100), 2440 (empty **4**, 55). Anal. Calcd for $C_{162}H_{138}Cl_4O_{24}$: C, 74.54; H, 5.29. Found: C, 74.82; H, 5.48.

4·CH_3CN. A solution of 20 mg of **4**·$(CH_3)_2NCOCH_3$ in 50 mL of 50 mol % CH_3CN in $C_6H_5CH_3$ was heated to reflux for 48 h and then cooled to 25 °C. Additional CH_3CN was added until precipitation occurred. The solid was filtered and dried: ^{1}H NMR for **4**·CH_3CN (500 MHz, $C_2D_2Cl_4$) δ −2.55 (s, 3 H, CH_3CN), 2.40–2.78 (m, 32 H, CH_2CH_2Ph), 3.80–4.81 (d, 8 H, inner OCH_2, J = 5 Hz), 4.70 (t, 8 H, methine, J = 7.5 Hz), 5.04 (s, 16 H, benzylic), 5.54–5.55 (d, 8 H, outer OCH_2, J = 5 Hz), 6.79 (s, 8 H, ArH), 7.17–7.36 (m, 56 H, ArH); MS (FABS, NOBA) m/e 2482 (M^+, 100), 2440 (empty **4**, 70). Anal. Calcd for $C_{162}H_{139}NO_{24}$: C, 78.36; H, 5.60. Found: C, 78.12; H, 5.44.

4·$CH_3(CH_2)_3OH$. Approximately 20 mg of **4**·$(CH_3)_2NCOCH_3$ in 50 mL of 50 mol % 1-butanol in toluene was heated to reflux for 48 h and then cooled to 25 °C. Upon cooling, a white precipitate formed, which was filtered and dried: ^{1}H NMR for **4**·$CH_3(CH_2)_3OH$ (500 MHz, $C_2D_2Cl_4$) δ −2.90 (t, 3 H, $CH_3(CH_2)_3OH$, J = 7 Hz), −2.21 (t, 1 H, ROH, J = 5 Hz), −0.70 (m, 2 H, $CH_3CH_2(CH_2)_2OH$), −0.55 (m, 2 H, $CH_3CH_2CH_2CH_2OH$), 1.0 (m, 2 H, CH_2 α to OH), 2.50–2.85 (m, 32 H, CH_2CH_2Ph), 4.09–4.10 (d, 8 H, inner OCH_2, J = 5 Hz), 4.85 (t, 8 H, methine, J = 7.5 Hz), 5.15 (s, 16 H, benzylic), 5.56–5.57 (d, 8 H, outer OCH_2, J = 5 Hz), 6.95 (s, 8 H, ArH), 7.18–7.36 (m, 56 H, ArH); MS (FABS, NOBA) m/e 2516 (M + 2, 100), 2442 (empty M^+, 35). Anal. Calcd for $C_{164}H_{146}O_{25}$: C, 78.28; H, 5.81. Found: C, 78.25; H, 5.79.

4·$CH_3CH_2COCH_3$. A solution of 20 mg of **4**·$(CH_3)_2NCOCH_3$ in 60 mL of 50 mol % 2-butanone was made in toluene. The mixture was heated to reflux for 48 h and then cooled to 25 °C. Upon cooling, a white precipitate formed, which was filtered and dried: ^{1}H NMR for **4**·$CH_3CH_2COCH_3$ (500 MHz, $C_2D_2Cl_4$) δ −2.90 (t, 3 H, $CH_3CH_2COCH_3$, J = 6.5 Hz), −2.0 (s, 3 H, $CH_3CH_2COCH_3$), 0.06 (q, 2 H, $CH_3CH_2COCH_3$), 2.48–2.80 (m, 32 H, CH_2CH_2Ph), 3.88–3.89 (d, 8 H, inner OCH_2, J = 5 Hz), 4.69 (t, 8 H, methine, J = 7.5 Hz), 5.05 (s, 16 H, benzylic), 5.50–5.51 (d, 8 H, outer OCH_2, J = 5 Hz), 6.92 (s, 8 H, ArH), 7.18–7.43 (m, 56 H, ArH); MS (FABS, NOBA) m/e 2513 (M^+, 100), 2440 (empty **4**, 70). Anal. Calcd for $C_{164}H_{144}O_{25}$: C, 78.34; H, 5.73. Found: C, 78.02; H, 5.44.

4·$CH_3CH_2O_2CCH_3$. A solution of 20 mg of **4**·$(CH_3)_2NCOCH_3$ in 50 mL of 1,4-diisopropylbenzene and 10 mL of ethyl acetate was heated to 120 °C for 72 h. Additional ethyl acetate was added, and the precipitate that formed was filtered and dried: ^{1}H NMR for **4**·$CH_3CH_2O_2CCH_3$ (500 MHz, $C_2D_2Cl_4$) δ −2.34 (t, 3 H, $CH_3CH_2O_2CCH_3$), −2.13 (s, 3 H, $CH_3CH_2O_2CCH_3$), 1.81 (q, 2 H, $CH_3CH_2O_2CCH_3$), 2.52–2.77 (m, 32 H, CH_2CH_2Ph), 4.02–4.03 (d, 4 H, inner OCH_2, southern hemisphere, J = 5 Hz), 4.15–4.16 (d, 4 H, inner OCH_2, northern hemisphere, J = 5 Hz), 4.78 (d of t, 8 H, methine, J = 7.5 Hz), 5.04 (s, 8 H, benzylic, southern hemisphere), 5.06 (s, 8 H, benzylic, northern hemisphere), 5.50–5.51 (d, 4 H, outer OCH_2, southern hemisphere, J = 5 Hz), 5.58–5.59 (d, 4 H, outer OCH_2, northern hemisphere, J = 5 Hz), 6.85 (s, 4 H, ArH, southern hemisphere), 6.87 (s, 4 H, ArH of northern hemisphere), 7.21–7.63 (m, 56 H, ArH); MS (FABS, NOBA) m/e 2530 (M + 2, 100), 2440 (empty **4**, 80). Anal. Calcd for $C_{164}H_{144}O_{26}$: C, 77.85; H, 5.69. Found: C, 77.83; H, 5.69.

4·$(CH_3)_2NCHO$. A solution of 20 mg of **4**·$(CH_3)_2NCOCH_3$ in 50 mL of 1,4-diisopropylbenzene and 10 mL of $(CH_3)_2NCHO$ was heated to 120 °C for 72 h and then cooled to 25 °C, and additional DMF was added until precipitation occurred. The solid was filtered and dried: ^{1}H NMR for **4**·$(CH_3)_2NCHO$ (500 MHz, $C_2D_2Cl_4$) δ −0.45 (s, 3 H, CH_3NCH_3CHO), 0.04 (s, 3 H, CH_3NCH_3CHO), 2.40–2.78 (m, 32 H, CH_2CH_2Ph), 3.95–3.96 (d, 8 H, inner OCH_2, J = 5 Hz), 4.75 (s, 1 H, formyl H of DMF), 4.79 (t, 8 H, methine, J = 7.5 Hz), 5.08 (s, 16 H, benzylic), 5.50–5.51 (d, 8 H, outer OCH_2, J = 5 Hz), 6.91 (s, 8 H, ArH), 7.23–7.43 (m, 56 H, ArH); MS (FABS, NOBA) m/e 2513 (M, 100), 2440 (empty **4**, 70). Anal. Calcd for $C_{163}H_{143}NO_{25}$: C, 77.83; H, 5.69. Found: C, 78.04; H, 5.92.

4·$CHCl_3$. A solution of 20 mg of **4**·$(CH_3)_2NCOCH_3$ in 50 mL of 1,4-diisopropylbenzene was heated to 200 °C for 24 h. The solution was cooled to 60 °C, 20 mL of $CHCl_3$ was added, and the mixture was stirred at that temperature for 48 h. Isooctane was added until precipitation occurred. The solid was filtered and dried: ^{1}H NMR for **4**·$CHCl_3$ (500 MHz, $C_2D_2Cl_4$) δ 2.40–2.78 (m, 32 H, CH_2CH_2Ph), 3.88–3.89 (d, 8 H, inner OCH_2, J = 5 Hz), 4.70 (t, 8 H, methine, J = 7.5 Hz), 5.02 (s, 16 H, benzylic), 5.29 (s, 1 H, $CHCl_3$), 5.53–5.54 (d, 8 H, outer OCH_2, J = 5 Hz), 6.81 (s, 8 H, ArH), 7.16–7.36 (m, 56 H, ArH); MS (FABS, NOBA) m/e 2560 (m, 100), 2440 (empty **4**, 55). Anal. Calcd for $C_{161}H_{137}Cl_3O_{24}$: C, 75.48; H, 5.35. Found: C, 75.13; H, 5.20.

Kinetics of Loss of $(CH_3)_2NCOCH_3$ from 4·$(CH_3)_2NCOCH_3$ in Various Solvents. Solutions prepared from 5–7 mg of **4**·$(CH_3)_2NCOCH_3$ dissolved in 0.5 mL of the deuterated solvents of Table III were placed in NMR tubes. The tubes were placed in the probe of the Bruker AM-500 NMR spectrometer, and the temperature of the probe was adjusted to 100 °C (±1 °C) after the probe temperature was calibrated with ethylene glycol.[11] Series of spectra (20–25) were recorded in which the signals of the upfield guest protons were lost due to their decomplexation. Table III records the first-order rate constants calculated from the spectral data.

Kinetics of Decomplexation of 4·Guests in $CDCl_2CDCl_2$. Solutions of 5–7 mg of **4**·guest (listed in Table IV) were dissolved in 0.5 mL of $CDCl_2CDCl_2$ that had been previously passed through a plug of neutral alumina. The tubes were placed in the probe of the NMR spectrometer at 100 °C, and 20–25 spectra were recorded at appropriate time intervals. The first-order decomplexation rate constants were calculated on the basis of the spectral changes that accompanied decomplexation and are listed in Table IV.

Kinetics of Complexation and Decomplexation Involving 4·$(CH_3)_2NCOCH_3$, 4·$CH_3CH_2O_2CCH_3$, 4·$CH_3CH_2COCH_3$, and 4·$CH_3C_6H_5$ in 1,2-$(CD_3)_2C_6D_4$ at Various Temperatures. Empty **4** (3 mg, 1.2×10^{-3} mmol) was dissolved in 0.6 mL of 1,2-$(CD_3)_2C_6D_4$ to give a 2 mM solution. Ethyl acetate (1.2 μL, 1.2×10^{-2} mmol) was added to the solution and was mixed well in an NMR tube. Series of 20–25 500-MHz spectra were taken at appropriate time intervals at three temperatures. The probe temperatures were calibrated against $HOCH_2CH_2OH$ as standard.[11] Similar host solutions were prepared for studies involving $(CH_3)_2NCOCH_3$ and $CH_3C_6H_5$ by adding 1.2 and 1.3 μL to respective 2 mM host solutions in 1,2-$(CD_3)_2C_6D_4$. Thus, with these three guests, a 10 molar equiv excess of guest to host was present. In the studies involving $CH_3CH_2COCH_3$, a 5:1 ratio of guest to host was employed. To 2 mM **4** in 1,2-$(CD_3)_2C_6D_4$ was added 6 μL of a 1 M solution of $CH_3CH_2COCH_3$ in 1,2-$(CD_3)_2C_6D_4$. Concentrations of free host and complex were determined from the integrals of the proton signals of the guest moved upfield by the complexation. Table V records the second-order rate constants for decomplexation (k_a, min^{-1} M^{-1}).

Decomplexation rate constants were determined similarly. A solution of 4 mg of each complex was dissolved in 0.6 mL of 1,2-$(CD_3)_2C_6D_4$, and 20–25 spectra were recorded at appropriate times and temperatures. The ratios of free host to complex were determined from the integrals of the inward-pointing OCH_2O protons for each species. The resulting k_d values are listed in Table VI, along with the derived association constants (K_a, M^{-1}). From these parameters and their dependence on temperature, $\Delta G°$, ΔH, and ΔS were calculated, as well as $\Delta G^‡$, $\Delta H^‡$, and $\Delta S^‡$ for association and dissociation. The values are recorded in Table VI.

Crystal Structure Determination of 4·$(CH_3)_2NCOCH_3$. The complex crystallizes from $(CH_3)_2NCOCH_3$–$CHCl_3$–$O(CH_2CH_2)_2O$ as colorless plates in the orthorhombic system *Pcan* (standard setting *Pbcn*). Unit cell dimensions are as follows: a = 18.226 (7), b = 24.286 (9), c = 49.822 (15) Å, v = 22234 Å^3, z = 4 (the molecule has C_2 symmetry). The crystal was examined on a Huber diffractometer, Mo Kα radiation, at 298 K. The structure was determined by direct methods. Refinement of 372 parameters (2 blocks, 249 + 123 parameters, 2199 reflections with $I > 2\sigma(I)$) has an agreement value, R, currently at 0.30. Of 11340 reflections, in a sphere limited by 2θ = 41°, only 1754 reflections had $I > 3\sigma(I)$. The $(CH_3)_2NCOCH_3$ guest incarcerated in the host was disordered. Its presence in a host:guest ratio of 1:1 was demonstrated by elemental analysis, FAB-MS, and ^{1}H NMR spectra proton signal ratios. The solvate:host ratio in the crystal must be high, judging from the volume of the unit cell. As many as 18 disordered solvate molecules

per host are indicated on a difference electron density map. Position parameters have been assigned for only 30 of the solvent atoms.

The hemicarcerand is in the wrapped conformation. The distance between the planes of the four oxygen atoms of each cavitand component is about 2.4 Å. The angle between normals to these two least-squares planes is 0.6°. The four oxygen atoms are ±0.04 Å from the least-squares plane through these four atoms. The distance between the oxygen atoms within a xylyl bridge ranges from 2.76 to 2.95 Å. The approximate squares formed by the four oxygen atoms of each cavitand are twisted with respect to each other by about 21° (defined by O–square midpoint–square midpoint–O).

Supplementary Material Available: Experimental details of the crystal structure determination, including tables of atom positions and their thermal parameters and bond lengths and angles (13 pages). Ordering information is given on any current masthead page.

Electrophilic Addition of Br_2 to Olefins in the Presence of Nucleophilic Trapping Anions. Implications for the Lifetimes of Bromonium Ion Intermediates Produced from Electrophilic Bromination of Olefins in Methanol

R. W. Nagorski and R. S. Brown*

Contribution from the Department of Chemistry, University of Alberta, Edmonton, Alberta, Canada T6G 2G2. *Received March 20, 1992*

Abstract: The product ratios for Br_2 or NBS additions to cyclopentene, cyclohexene, tetramethylethylene, and styrene in MeOH containing varying concentrations of added N_3^- or Br^- have been determined with an aim of determining the lifetimes of the bromonium ion intermediates. On the basis of the ratio of trans bromo azide to methoxy bromide products, the partitioning rate constant ratios (k_{N_3}/k_{CH_3OH}) for the four olefins are 5.9, 4.9, 9.3, and 2.7 M^{-1}, respectively. That the far better nucleophile (N_3^-) does not lead to a marked increase in product formation relative to solvent suggests that both species capture a highly reactive intermediate in a non-activation-limited process. Assuming that the N_3^- reacts with the intermediate with a diffusion-limited rate constant of 10^{10} M^{-1} s^{-1}, the respective lifetimes of the ions produced from bromination of the four olefins are 5.9×10^{-10}, 5.0×10^{-10}, 9.3×10^{-10}, and 2.7×10^{-10} s, respectively. On the basis of existing comparisons, these values indicate the following: the cyclic olefins produce ions that live about 100 times longer than a secondary carbocation; tetramethylethylene gives a bromonium ion that lives ~10 times longer than a tertiary cation; and styrene gives an ion (bromonium or β-bromo cation) that is ~40-fold longer lived than the 1-phenylethyl cation. In the case of Br_2 or NBS addition to cyclohexene in the presence of varying $[Br^-]$, the ratio of the trans dibromide to methoxy bromide product tends to zero as $[Br^-] \rightarrow 0$. This indicates that the trans dibromide cannot be formed by ion pair collapse. The solvolysis of *trans*-2-bromocyclohexyl trifluoromethanesulfonate in MeOH containing N_3^- or Br^- produces significantly less azide or bromide capture product than does electrophilic addition of Br_2 or NBS to cyclohexene under the same conditions, suggesting that the ions produced in the two cases are not identical.

Introduction

The electrophilic bromination of olefins is a well-studied reaction[1] that has recently attracted renewed interest. The generally accepted mechanism is given in eq 1. In protic solvents at low $[Br_2]$, the reaction is first order in $[Br_2]$ and proceeds via a 1:1 charge-transfer complex (CTC). At higher $[Br_2]$ or in nonprotic

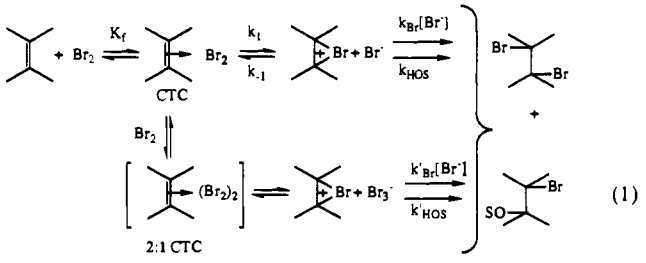

(1)

solvents, terms second order in $[Br_2]$ are seen and interpreted as a Br_2-assisted ionization of the 1:1 CTC (perhaps via a 2:1 CTC) to produce a bromonium ion tribromide.[2] The more recent work has centered on structural and NMR characterization of a stable bromonium ion,[3] determining the circumstances where reversible formation of the ions occurs[2,4] and determining the importance of nucleophilic solvent assistance in bromination.[4f]

In some cases, bromonium ions can be studied by NMR under stable ion conditions.[5] However, because of the general instability of three-membered bromonium ions toward nucleophilic attack, very little information exists about the characteristics of these ions in solution. One of these is the lifetime, about which virtually no data exist other than the fact that the ion must live sufficiently long to allow a translocation of Br^- from where it is formed after the ionization of the CTC to where it attacks the carbon to form

(1) (a) Schmid, G. H.; Garrat, D. G. *The Chemistry of Double-Bonded Functional Groups*; Patai, S., Ed.; Wiley: New York, 1977; Suppl. A, Part 2, p 725. (b) De la Mare, P. B. D.; Bolton, R. *Electrophilic Additions to Unsaturated Systems*, 2nd ed.; Elsevier: New York, 1982; pp 136–197. (c) V'yunov, K. A.; Guniak, M. I. *Russ. Chem. Rev. (Engl. Transl.)* **1981**, *50*, 151–163. (d) Ruasse, M. F. *Acc. Chem. Res.* **1990**, *23*, 87.

(2) Brown R. S.; Slebocka-Tilk, H.; Bennet, A. J.; Bellucci, G.; Bianchini, R.; Ambrosetti, R. *J. Am. Chem. Soc.* **1990**, *112*, 6310 and references therein.

(3) (a) Slebocka-Tilk, H.; Ball, R. G.; Brown, R. S. *J. Am. Chem. Soc.* **1985**, *107*, 4505. (b) Bennet, A. J.; Brown, R. S.; McClung, R. E. D.; Aarts, G. M.; Klobukowski, M.; Santarsiero, B. D.; Bellucci, G.; Bianchini, R. *J. Am. Chem. Soc.* **1991**, *113*, 8532.

(4) (a) Brown, R. S.; Gedye, R.; Slebocka-Tilk, H.; Buschek, J.; Kopecky, K. R. *J. Am. Chem. Soc.* **1984**, *106*, 4515. (b) Bellucci, G.; Chiappe, C.; Marioni, F. *J. Am. Chem. Soc.* **1987**, *109*, 515. (c) Bellucci, G.; Bianchini, R.; Chiappe, C.; Marioni, F.; Spagna, R. *J. Am. Chem. Soc.* **1988**, *110*, 546. (d) Bellucci, G.; Bianchini, R.; Chiappe, C.; Marioni, F.; Ambrosetti, R.; Brown, R. S.; Slebocka-Tilk, H. *J. Am. Chem. Soc.* **1989**, *111*, 2640. (e) Ruasse, M.-F.; Motallebi, S.; Galland, B.; Lomas, J. S. *J. Org. Chem.* **1990**, *55*, 2298. (f) Ruasse, M.-F.; Motallebi, S.; Galland, B. *J. Am. Chem. Soc.* **1991**, *113*, 3440.

(5) Olah, G. A. *Halonium Ions*; Wiley Interscience: New York, 1975 and references therein.

0002-7863/92/1514-7773$03.00/0